The patterns of soil nitrogen stocks and C:N stoichiometry under impervious surfaces in China

Qian Ding[1], Hua Shao[2], Chi Zhang[2, 1, 3, *], Xia Fang[4]

[1]Shandong Provincial Key Laboratory of Water and Soil Conservation and Environmental Protection, College of Resources and Environment, Linyi University, Linyi, 270600, China.
[2]State Key Laboratory of Desert and Oasis Ecology, Xinjiang Institute of Ecology and Geography, Chinese Academy of Sciences, Urumqi, 830011, China.
10 [3]Research Center for Ecology and Environment of Central Asia, Chinese Academy of Sciences, Urumqi, 830011, China.
[4]Xinjiang Institute of Engineering, Urumqi, 830091, China.

Correspondence to: Chi Zhang (zc@ms.xjb.ac.cn)

Abstract. Accurate assessment of soil nitrogen (N) storage and carbon (C):N stoichiometry under impervious

15 surface areas (ISAs) is key to understanding the impact of urbanization on soil health and the N cycle. Based on 888 soil profiles from 148 sampling sites in 41 cities across China, we estimated the country's N stock (100 cm depth) in the ISA soil to be 96.88 Tg N with a mean N density (N_{ISA}) of 0.59±0.35 kg m^{-2}, which was significantly lower (at all depths) than the soil N density (N_{PSA} = 0.83±0.46 kg m^{-2}) under the reference permeable surface areas (PSAs). Both N_{ISA} and N_{PSA} were higher than the mean N density of natural soils in

20 China. These findings indicate that urbanization did not cause soil N loss, but the conversion of PSA to ISA could reduce soil N by 29%. In comparison with the PSA, the ISA had a lower soil organic carbon (SOC) to N ratio (SOC:N) of 10.33±2.62 and a significant C–N correlation, showing no signs of C–N decoupling as suggested by the previous studies that might have been misled by the extremely high total C:total N ratio in the ISA soil. Moreover, the ISA had smaller variances in the SOC:N ratio than did the PSA, indicating

25 convergence of soil C:N stoichiometry due to ISA conversion. Unlike natural soil, the SOC:N_{ISA} was negatively correlated with temperature. Unlike the vertical pattern in natural permeable soils, whose N density declined faster in the upper soil layers than in the lower layers, N_{ISA} decreased linearly with depth. In the spatial map of China's N_{ISA}, the highest N_{ISA} was found in the northeast and the lowest in the southeast, and the highest SOC:N ratio was found in the Yangtze River Delta. This study revealed the unique spatial

30 patterns of soil N under the ISA in China, which could potentially improve our capacity to assess and model urban biogeochemical cycles.

1 Introduction

Nitrogen (N) is an essential nutrient that regulates ecosystem structure and function and maintains nutrient cycling (Fowler et al., 2013). It affects ecosystem carbon sequestration in various ways (Vitousek and

35 Howarth, 1991), and the C:N stoichiometry conveys a rough measure of the mineralization and humification of soil organic matter (SOM) (Chapin et al., 2011). Currently, global ecosystem structure and functions are

intensively disrupted by urbanization, especially the rapid expansion of impervious surface area (ISA). ISA covers approximately 5.8×10^5 km^2 global land area (Lehmann and Stahr, 2007) and was projected to triple during 2000–2030 (Seto et al., 2012). It has been suggested that the expansion of ISA blocks soil–atmosphere

40 carbon/water exchanges, alters the physicochemical properties of soil, and seriously disrupts soil biogeochemical processes (Wei et al., 2014a; Yu et al., 2019). N loss from disturbed urban soils may cause groundwater N contamination (Li et al., 2022). Thus, there is an urgent need to study N_{ISA} and SOC: N_{ISA} patterns to provide a solid basis for assessing the potential risk of N loss and other negative impacts on urban ecosystems (Pereira et al., 2021).

45 Due to the difficulties in sampling beneath impervious surfaces, our knowledge about the biogeochemical processes in sealed soils is still very limited. Although the knowledge gap has gained more attention recently, most of the studies in ISAs have focused on the soil organic carbon (SOC) pool but have generally overlooked the soil N pool (Yan et al., 2015; Bae and Ryu, 2020; Cambou et al., 2018; Short et al., 1986). These studies showed that soil sealing not only causes a large amount of SOC loss but also alters the structure of the SOC

50 pools, indicating profound changes in soil carbon (C) processes (Wei et al., 2013; Raciti et al., 2012; Ding et al., 2022). To date, only a few isolated studies from seven cities (three in China, three in Europe and one in the USA) have reported the soil N content/density under ISA (N_{ISA}) (Table 1). All of these studies indicated that N_{ISA} was lower than the N content/density (N_{PSA}) in pervious surface area (PSA). Two of them found extremely high C:N ratios in ISA (164 vs. 19 in PSA soil, 12.44 vs. 6.99 in PSA, respectively), suggesting

55 decoupling of C and N processes as the result of soil sealing (Raciti et al., 2012; O'riordan et al., 2021). A study from Nanjing city, China, however, found that ISAs had a lower C:N ratio than PSAs (Wei et al., 2014a).

There were two major limitations in previous studies: (1) they sampled only the topsoil or upper soil layers (Table 1) and thus could not obtain a complete picture of the vertical distribution pattern of the N_{ISA}; and (2)

60 they focused on a single city and used different sampling/analysis methods, which made it difficult to compare the datasets to the real spatial distribution pattern of the N_{ISA} pool at large scales. Without abundant large–scale N_{ISA} data, it will be difficult to assess the global N_{ISA} pool size, to examine whether soil sealing decouples the C and N processes (which is a sign of ecosystem degradation), and to study how the N_{ISA} and the coupled C processes are influenced by climatic, ecological, and socioeconomic factors across large areas.

65 To address these issues, we investigated the patterns of China's N_{ISA} pool and SOC:N_{ISA} (SOC:N ratio of the ISA) based on 148 observations from 41 major cities across China (sampled at 100 cm depth and 20 cm intervals). The objectives of this study were to (a) compare N_{ISA} with N_{PSA}, (b) reveal the spatial pattern of N_{ISA} and SOC:N_{ISA}, and (c) identify the environmental factors correlated with N_{ISA} and SOC:N_{ISA} and discuss the underlying mechanism. Justifications of the study design: China's urbanization rate is twice the global

70 average, and approximately 2/3 of its urban area is occupied by ISA, which is also higher than the global average (Kuang, 2019). There are also relatively more previous N_{ISA} studies in Chinese cities than in other countries (Table 1), which makes it easier to evaluate our results. We chose to use the SOC:total N ratio

rather than the total C:total N ratio to analyse the C:N stoichiometry because the content of soil inorganic C under impervious surfaces is likely altered by anthropogenic C from construction materials (Zhao et al., 2017; O'riordan et al., 2021). SOC:total N has been widely used as an indicator of soil C:N stoichiometry in previous studies (Schroeder et al., 2022; Lu et al., 2023; Tian et al., 2010; Yang et al., 2021; Wei et al., 2014a).

Table 1: Compilation of soil N_ISA studies

City, country	Previous studies				This study		
	N density (kg m⁻²)	N content (g kg⁻¹)	Depth (cm)	References	N density (kg m⁻²)*	N content (g kg⁻¹)*	Depth (cm)
Beijing, China	NA	0.61	0–10	(Zhao et al., 2012)	0.08±0.02	0.34±0.06	0–20
	NA	0.54	10–20		0.08±0.02	0.34±0.06	0–20
	NA	0.42	20–30		0.09±0.02	0.4±0.11	20–40
	NA	0.26	30–40		0.09±0.02	0.4±0.11	20–40
	NA	0.37	0–15	(Hu et al., 2018)	0.08±0.02	0.34±0.06	0–20
Nanjing, China	NA	0.49	0–20	(Wei et al., 2014b)	0.38±0.05	0.13±0.15	0–20
Yixing, China	0.25	NA	0–20	(Wei et al., 2014a)	0.15±0.01	NA	0–20
New York, USA	0.014	NA	0–15	(Raciti et al., 2012)	0.10±0.06	NA	0–15
Lancaster, UK	NA	2.08	0–10	(Pereira et al., 2021)	0.07±0.04	NA	0–10
Greater Manchester, UK	0.081	NA	0–10	(O'riordan et al., 2021)	0.07±0.04	NA	0–10
Toruń, Poland	0.027	0.17	15–25 or 10–20	(Piotrowska-Długosz and Charzyński, 2015)	0.12±0.08	NA	0–20

*±1SD

2 Materials and methods

80   **2.1 Soil sampling**

The soil samples were collected from 148 sample sites in 41 cities that were evenly distributed across mainland China except for the Tibetan Plateau during 2013–2014 (Figure 1). Depending on the city size, multiple sample sites were identified in each city. Each site belonged to a separate city district, i.e., the soil samples were taken from 148 different city districts across China. The sample sites included various ISA

85   types (roads, elevated piers, floor buildings, etc.) and PSA types (trees, shrubs, herbs, bare ground, vegetable plots, etc.). Detailed descriptions of the cities and sample sties can be found in (Ding et al., 2022; Ding et al., 2023).
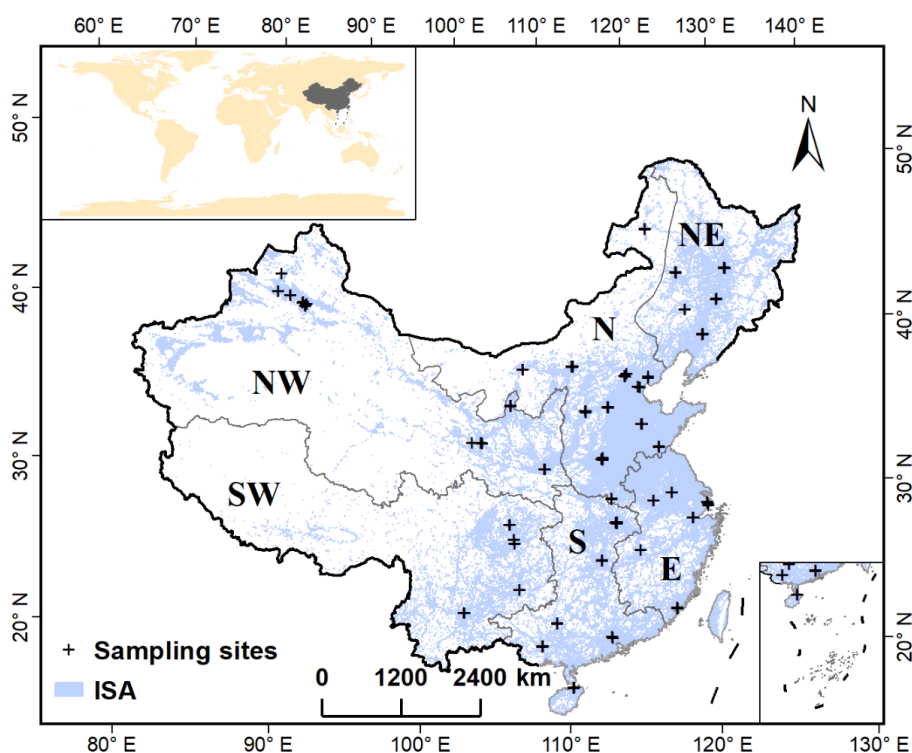
Figure 1: Spatial distribution of ISA sample points. E: eastern China, S: southern China, N: northern China, NE: northeastern China, NW: northwestern China, SW: southwestern China.

90   At each sample site, 3 representative ISA sampling plots, more than 10 m apart from each other, were randomly selected. In addition, three paired sampling plots in adjacent PSAs were randomly selected for comparison. In each plot, a 100 cm depth profile pit was dug, and the soil profile was sampled at 20 cm intervals to the 100 cm depth with a 100 cm^3 ring knife. A total of 4356 soil samples were eventually collected from 888 soil profiles. These samples (ID# XJBIZC0001–XJBIZC4356) are currently stored in the herbarium

95   of the Xinjiang Institute of Ecology and Geography, Chinese Academy of Sciences.

2.2 Soil physical and chemical analyses

The SOC density of the samples was reported in a previous study (Ding et al., 2022). In this study, soil bulk density (BD) and N content were measured for each soil sample. Soil samples inside the ring knife were dried at 105 °C, and soil bulk weight (BD) (g cm⁻³) was measured, while the rest of the samples were air dried and

100   passed through a 0.15 mm sieve, and the N content (g kg⁻¹) was measured by Kjeldahl digestion (Bremner and Mulvaney, 1982). The N density (kg m⁻²) per 20 cm soil layer was calculated according to Eq. 1, and the N density for the entire 100 cm profile was obtained by summing the N density per 20 cm soil layer (Eq. 2).

$$N_i = \frac{\text{N content}_i \times \text{BD}_i \times 20}{100},\tag{1}$$

$$N_{100cm} = \sum_{i=1}^{n} N_i,\tag{2}$$

105   where i represents soil layer i (20 cm depth), i = 1, 2......5.

2.2 Auxiliary data
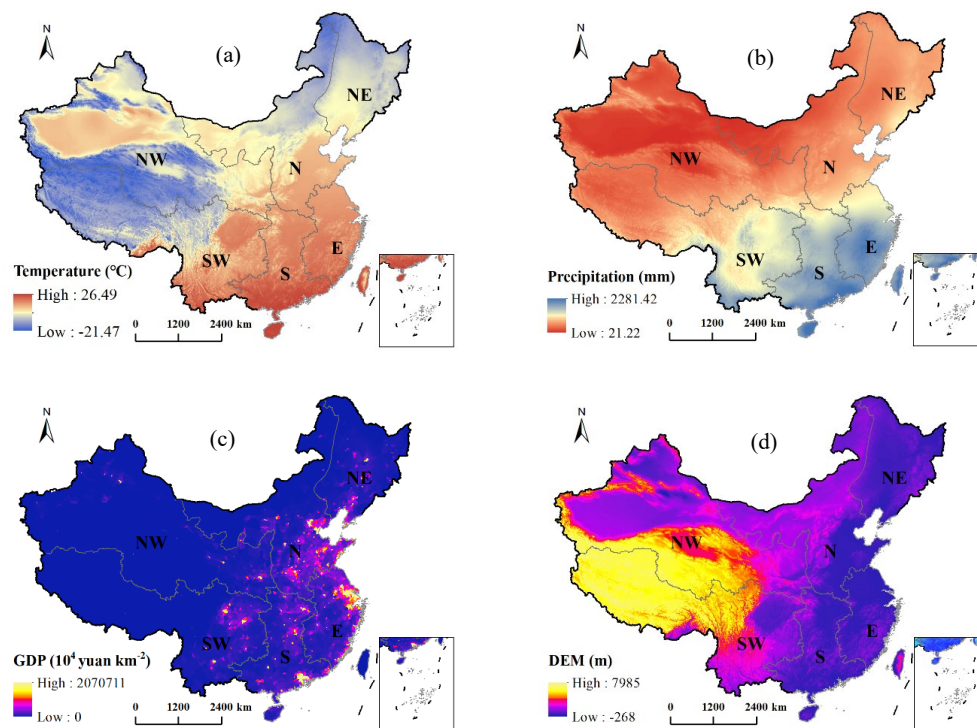
Figure 2: The 4 spatial datasets of China used in this study, including (a) annual precipitation normal (1981–2010), (b) air temperature normal (1981–2010), (c) gross domestic product (GDP), and (d) digital elevation model. E: eastern China, S: southern China, N: northern China, NE: northeastern

110   **China, NW: northwestern China, SW: southwestern China.**

Auxiliary data were used to investigate the environmental factors that influence the spatial pattern of N_{ISA} and the SOC:N ratio in China. Climate normality data (multiyear mean annual temperature, multiyear mean annual precipitation) for 1981–2010, digital elevation model (DEM) data and gross domestic product (GDP) data in 2015 were obtained from the Resource and Environment Science and Data Center, Chinese Academy

115 of Sciences (http://www.resdc.cn/). These 1 km resolution raster maps were rescaled to 30 m resolution using linear interpolation to match the spatial resolution of the ISA map (Figure 2). The ISA distribution map (30 m resolution) of China (Figure 1) was obtained from the Global ISA data product (Zhang et al., 2020).

2.3 Comparing N_{ISA} and N_{PSA}, SOC:N_{ISA} and SOC:N_{PSA}

A paired T test (2 tailed) was used to determine the difference between N_{ISA} and N_{PSA} and the difference

120 between SOC:N_{ISA} and SOC:N_{PSA} (SOC:N ratio of the PSA). The C:N stoichiometry, i.e., the SOC:N ratio, shows the connection between the C process and N process. An extremely high SOC:N_{ISA} in comparison with the reference SOC:N_{PSA} indicates C–N decoupling due to soil sealing (Raciti et al., 2012). The coefficient of variation (CV) was calculated to compare the variations in SOC:N between the ISAs and PSAs (Ding et al., 2022). A lower CV of SOC:N in ISA than in PSA would indicate that soil sealing has reduced

125 C:N stoichiometry variation, thus confirming the urban ecosystem convergence theory (Pouyat et al., 2003). Finally, spatial trend analyses were conducted to reveal the spatial variation patterns of N_{ISA}.

2.4 Investigating the vertical pattern of N_{ISA}

Unlike other studies that focused on topsoil, our multiple–layer soil sampling data made it possible to study the vertical pattern of N_{ISA} to a 100 cm depth. The proportions of N stored in the 0–20 cm depth, 0–40 cm

130 depth, 0–60 cm depth, and 0–80 cm depth to the total (100 cm depth) N stock in each sample profile were calculated and plotted against the soil depth to reveal the vertical distribution pattern of N_{ISA} and N_{PSA}. Based on these data, we could model how N storage changed with soil depth. According to Yang et al. (2017) (Yang et al., 2007), 46% of the N stock (in 1 m depth) of natural soil is stored in the top 0–30 cm soil, and 68% of the N stock is stored in the top 0–50 cm, translating into a power function fitting model:

135 $$N_{Natural}\%_d = 130 - 130 \times 0.99^d, \tag{3}$$

where $N_{Natural}\%$ is the proportion of N stored to depth d in natural soil in China.

2.5 Predicting the distribution patterns of N_{ISA} and C:N stoichiometry

Following Zhang et al. (2021) (Zhang et al., 2021), we used random forests to predict the N densities across China. The predictors included multiyear mean annual temperature, multiyear mean annual precipitation,

140 DEM and GDP. In the model, 90% of the N densities were randomly sampled at each split, and 500 trees were grown. Model prediction was repeated 100 times to obtain the average results. In addition, the spatial pattern of the SOC:N_{ISA} was calculated from the predicted N density and previous SOC$_{ISA}$ (SOC under ISA)

density datasets (Ding et al., 2022). Random forests were built using the randomForest package in R (Liaw and Wiener, 2002).

145   To evaluate the model performance, we evaluated the strength of prediction using a five–fold cross–validation method implemented with the R package "caret" (Kuhn, 2020; Gao et al., 2022). Based on this method, the entire dataset was randomly split into five groups. We calculated the linear relationship between the observed validation data (10% of the dataset by random sampling) and predicted data that were estimated based on training data (90% of the dataset by random sampling) 100 times with the model. The R^2 and root

150   mean square error were used to evaluate model accuracy and performance (Shcherbakov et al., 2013).

3 Results

3.1 N densities under ISA and PSA in China

The national mean N_{ISA} density in the 100 cm soil profile was 0.59 ± 0.35 kg m^{-2} (mean$\pm$1 SD), ranging from 0.08–1.88 kg m^{-2} with a median value of 0.48 kg m^{-2}. Paired t tests showed that the N_{ISA} was significantly

155   (approximately 30%) lower ($P<0.01$) than the reference N_{PSA} (Figure 3a). Moreover, the N_{ISA} was lower than the reference N_{PSA} at all soil depths.

SOC:N_{ISA} (10.33 ± 2.62) was significantly lower than SOC:N_{PSA} (10.93 ± 3.19) (Figure 3b). Moreover, N_{PSA} and SOC$_{PSA}$ were significantly correlated (R=0.893, P<0.01), and N_{ISA} and SOC$_{ISA}$ were also significantly correlated (R=0.926, P<0.01). There were no signs of C–N decoupling according to our data.
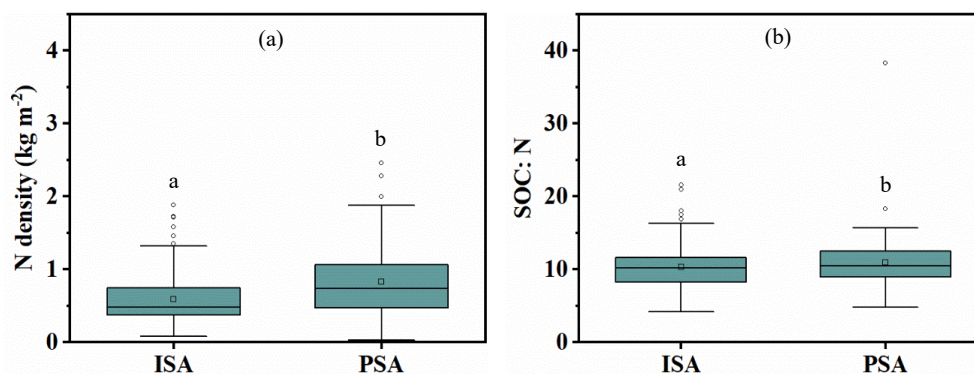
160   **Figure 3: Comparing soil N density (a) and SOC:N (b) in the ISA and the reference PSA. The square box shows median and quad values, the inner small rectangle is the mean value, and the letters indicate the significance of the difference among the groups.**

3.2 Spatial variation and spatial trend analysis

165   The mean intra–city CV of SOC:N$_{ISA}$ was larger (but insignificantly) than that of SOC:N$_{PSA}$, indicating that ISAs had similar or slightly higher SOC:N variations than PSAs within a city. However, the inter–city CV of SOC:N was 24% lower in ISAs (16%) than in PSAs (21%) (Figure 4), indicating that soil sealing resulted in more homogeneous soil C:N stoichiometry among the cities.
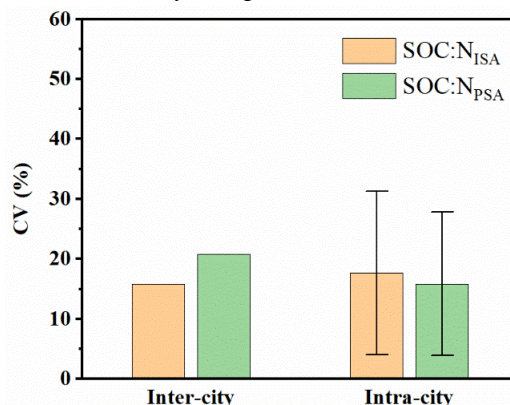
Figure 4: Comparing the mean intra–city CV and the inter–city CV of the SOC:N ratios between the
170   **ISAs and PSAs among 41 cities in China. The inter–city CVs were calculated based on city–level SOC:N, whereby the mean SOC:N value of each city was treated as a sample.**

The spatial trend analysis of the N$_{ISA}$ showed a slow decline followed by a rapid increase in the north–south direction and a rapid decline followed by a rapid increase in the east–west direction (Figure 5a); the spatial trend analyses of the N$_{PSA}$ produced similar concave lines in both the north–south and the east–west directions
175   but with a more drastic initial decline in the north–south direction and a flatter trend in the east–west direction (Figure 5b). The spatial trend analysis of SOC:N$_{ISA}$ showed a rapid increase in the north–south direction and a rapid decrease followed by a slow increase in the east–west direction (Figure 5c); the spatial trend analysis of SOC:N$_{PSA}$ showed a slow increase in the north–south direction and a slow decrease in the east–west direction (Figure 5d). According to the spatial trend analyses, the change rate of SOC:N$_{ISA}$ was significantly
180   higher than that of SOC:N$_{PSA}$, which was consistent with the results of inter–city CV.
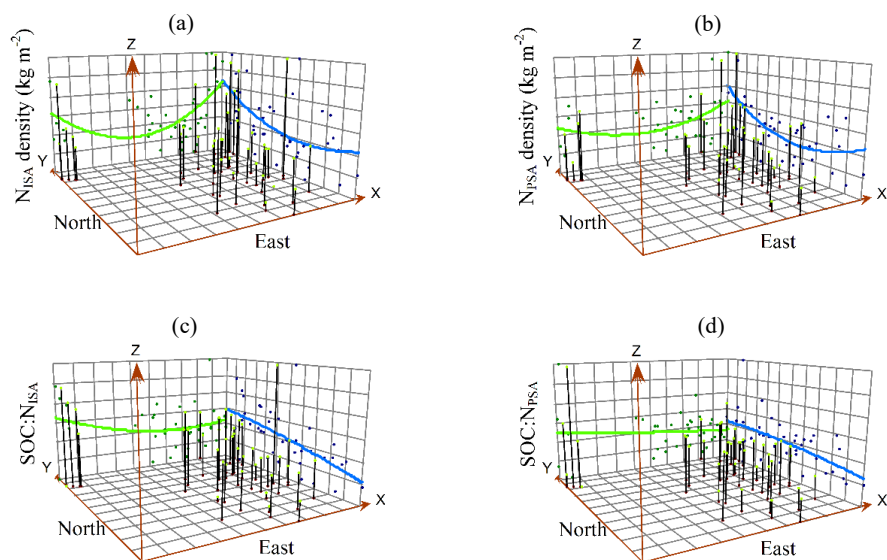
Figure 5: The variation trend of N and SOC:N under the two surfaces.

3.4 Vertical distribution pattern of N_{ISA}

In this study, the vertical profiles of soils under ISAs were systematically sampled and analysed at 20 cm intervals to a 100 cm depth, and the storage of N_{ISA} increased linearly with soil depth (Figure 6). This linear distribution pattern was evident at the national scale ($R^2 = 1$, P < 0.001), and the vertical distribution pattern of N_{ISA} in China can be described by a linear model (Eq. 4):

$$N_{ISA}\%_d = d + 2.31, \tag{4}$$

where $N_{ISA}\%\ d$ (%) is the percentage of total N storage (of 100 cm depth) stored in the top d (cm) depth of the soil.
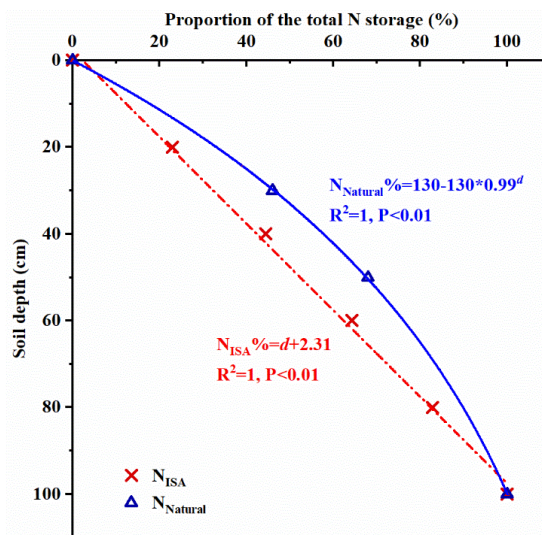
Figure 6: Comparing the vertical distribution pattern of N between the sealed soil (N_{ISA}) and the natural soil ($N_{natural}$) in China (refer to Section 2.4 Equation 3) (Yang et al., 2007).

3.5 Mapping of the N pool and SOC:N ratio under ISAs in China

The cross–validation indicated that the random forest model produced the N_{ISA} distribution in China with a high R^2 of 0.84 (Figure 7). Figure 8 shows the model–produced N_{ISA} map of China and the SOC:N_{ISA} map of China that was estimated based on the N_{ISA} map and the SOC_{ISA} map of China produced by Ding et al. (2022) (Ding et al., 2022).
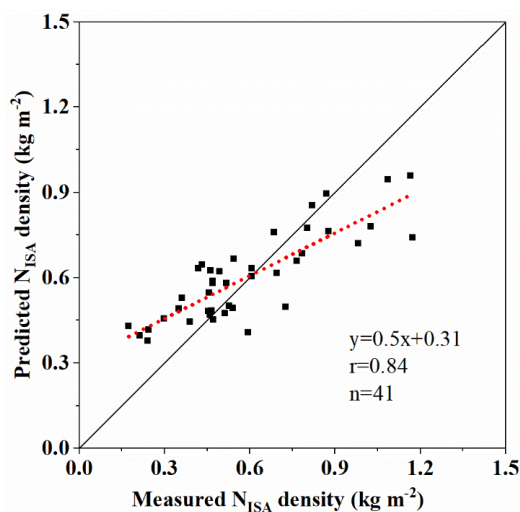
Figure 7: Cross–validation of the modelled N_{ISA} density in 41 cities in China.

According to the N_{ISA} map, approximately 96.88 Tg N is stored under ISAs in China, covering an area of 1.68×10^5 km^2. The spatial heterogeneity of the N_{ISA} density is strong, with the northeast having a higher

200 N_{ISA} density than other regions (Figure 7a). To facilitate spatial analysis, we divided the country into six
subregions – the northeast, north, northwest, east, south, and southwest, according to geography, climate, and
socioeconomics following Ding et al. (2022) (Ding et al., 2022) (Figure 1). The highest N_{ISA} density of
0.8±0.13 kg m^{-2} was found in the northeast, while the lowest N_{ISA} density of 0.47±0.06 kg m^{-2} was found in
the south (Figure 7c). The northern region accounted for the largest share (33%) of the N_{ISA} stock in China

205 (Figure 8d), mainly due to its large area of impervious surfaces.

The SOC:N_{ISA} map showed high SOC:N_{ISA} in the Yangtze River Delta and low SOC:N_{ISA} in central and
southern China (more precisely, in Hubei and Hunan Provinces), with a mean SOC:N_{ISA} ratio of 10.63±3.1
across China (Figure 8b). The eastern region had the highest SOC:N_{ISA} ratio of 13.19±3.88, while the
southern region had the lowest SOC:N_{ISA} of 8.53±1.74 (Figure 8e).
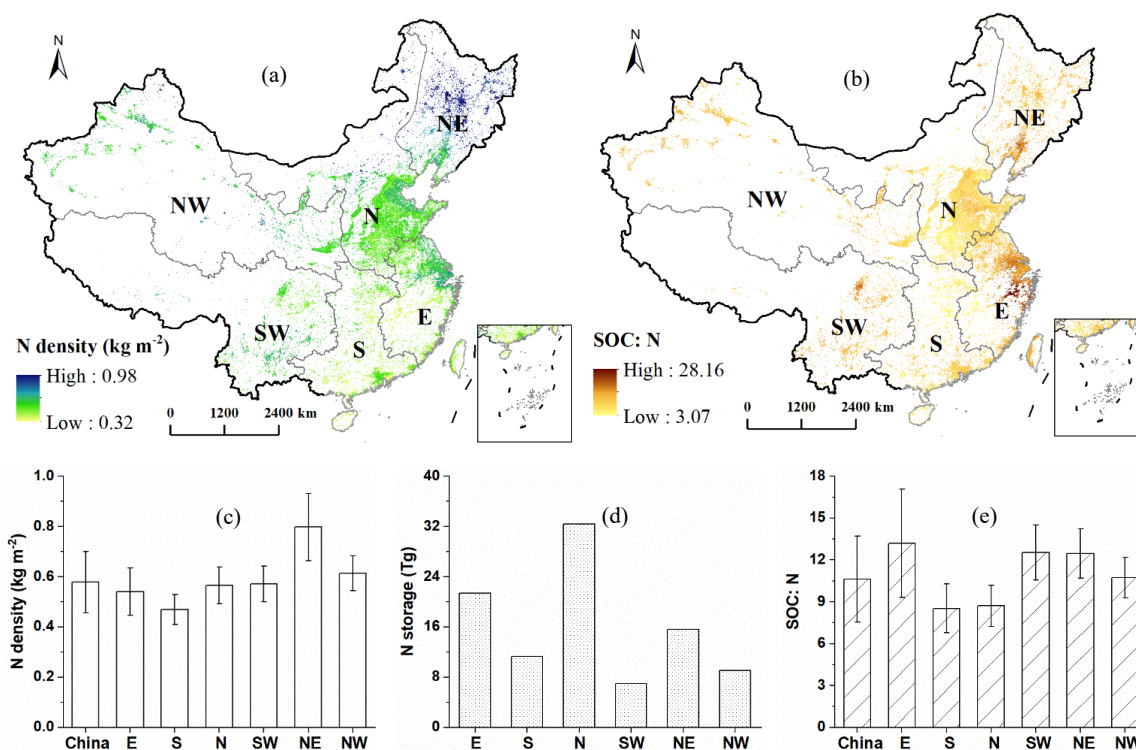
210 **Figure 8: The spatial patterns of N_{ISA} and SOC:N_{ISA} in China and the subregions. (a) N_{ISA} density map**
of China (Ding et al., 2023), (b) SOC:N_{ISA} map of China (Ding et al., 2023), (c) comparing the mean
N_{ISA} density in China and the subregions, (d) comparing the N_{ISA} storage in subregions, and (e)
comparing the SOC:N_{ISA} in China and the subregions. E: eastern China, S: southern China, N:
northern China, NE: northeastern China, NW: northwestern China, SW: southwestern China.

215 **4 Data availability**

The dataset "Observations of soil nitrogen and soil organic carbon to soil nitrogen stoichiometry under the impervious surfaces areas (ISA) of China" includes N density, N content, BD, SOC:N, and other related data under ISA and PSA. It also contains geographical coordinates of sampling locations, as well as spatial pattern layer files of N_{ISA} density and SOC:N_{ISA} in China. This dataset is available from the National Cryosphere

220 Desert Data Center (http://www.ncdc.ac.cn/portal/metadata/review/04cee3f5-64bb-4b22-9368-ee1c55f9c2bb?lang=en) (Ding et al., 2023).

5 Discussion

5.1 Comparing the N density and C:N stoichiometry in ISA soil with those in natural soils

Our results were comparable to or moderately lower than the previously reported topsoil (0–20 cm) N_{ISA}

225 contents/densities in Chinese cities, including Beijing (0.34±0.06 g kg^{-1} vs. 0.37–0.61 g kg^{-1}) (Hu et al., 2018; Zhao et al., 2012), Nanjing city (0.13±0.15 g kg^{-1} vs. 0.49 g kg^{-1}) (Wei et al., 2014b) and Yixing city (0.15±0.01 kg m^{-2} vs. 0.25 kg m^{-2}) (Wei et al., 2014a) (Table 1). Our observed N_{ISA} content (0.4 g kg^{-1}) in the 20–40 cm soil layer in Beijing was also comparable to the reports by Zhao et al. (2012) (0.26–0.42 g kg^{-1}) (Zhao et al., 2012). Outside China, the reported topsoil (0–10 cm) N_{ISA} density in Greater Manchester, UK

230 (0.081 kg m^{-2}), was comparable to our estimated mean N_{ISA} density in 0–10 cm (0.07±0.04 kg m^{-2}) in China (O'riordan et al., 2021), but the reported N_{ISA} in New York, USA and Toruń, Poland, was much lower than our results and the reports from other Chinese city studies (Table 1) (Raciti et al., 2012; Piotrowska-Długosz and Charzyński, 2015).

Compared with previous assessments of China's soil N stock, N_{ISA} accounted for 0.95–1.44% of the total soil

235 N pool in China (Zhang et al., 2021; Xu et al., 2020). The N_{ISA} pool size (96.88 Tg) exceeded the vegetation N of scrubland (8.1–50 Tg) (Xu et al., 2020) and grassland (48.8 Tg) (Zhang et al., 2021) in China. The N_{ISA} density (0.58±0.12 kg m^{-2}) was lower than that of natural soil and equivalent to 53–69% of the national average (Yang et al., 2007; Xu et al., 2020). The N densities in ISA soil (0.59±0.35 kg m^{-2}) were lower than those in other ecosystems, such as forest (1.29 kg m^{-2}), farmland (1.13 kg m^{-2}), and grassland (1.11 kg m^{-2})

240 (Xu et al., 2020), indicating that ISA construction resulted in N loss. Previous studies ignored the impacts of ISAs (Tian et al., 2006; Yang et al., 2007) and thus might have overestimated China's soil N pool size. Our estimated SOC:N_{ISA} (10.33±2.62) in China also matched the previously observed SOC:N_{ISA} (10.8) in Yixing city, China (Wei et al., 2014a).

It has been suggested that different terrestrial ecosystems may have similar SOC:N ratios (Yang et al., 2021).

245 This study showed that the SOC:N_{ISA} (10.33±2.62) was only slightly lower than the SOC:N_{PSA} (10.93±3.19) in urban ecosystems but much higher than the SOC:N ratios of natural ecosystem soils such as forests (8.21), croplands (8.18), and grasslands (7.7) (Xu et al., 2020; Tang et al., 2018). Therefore, it is possible that the

C:N stoichiometry could remain relatively stable within the same land–use type (natural ecosystems, urban areas, etc.) but might differ significantly among different natural or human–disturbed land–use types.

5.2. The SOC:N stoichiometry analysis showing no sign of C–N decoupling in the ISA soil

The above comparison indicates that ISA soil has a higher SOC:N than natural soils. A study in New York City reported that the N density in the ISA was 95% lower than that in the PSA, leading to an extremely high soil total C:total N ratio (Raciti et al., 2012; Majidzadeh et al., 2017). Therefore, Raciti et al. (2012) suggested that paving decouples the C and N cycles. Our observations, however, showed that the soil N of ISA was only 30% lower than that of PSA, and the $SOC:N_{ISA}$ was lower than the $SOC:N_{PSA}$ in China. Furthermore, there was a significant positive correlation (R=0.926, P<0.01) between N and SOC in ISA soil. Similarly, Wei et al. (2014a) found that $SOC:N_{ISA}$ was lower than $SOC:N_{PSA}$ in Yixing city, China (Wei et al., 2014a), and O'Riordan et al. (2021) found a significant positive correlation between N and C in ISA soil in Greater Manchester, UK, even though they also observed an increased total C:total N ratio in ISA soil compared to PSA soil (O'riordan et al., 2021). There were no signs of C–N decoupling according to our data and others (O'riordan et al., 2021; Wei et al., 2014a). It is possible that the extremely high C:N ratio observed in previous studies might be merely caused by anthropogenic C inputs that partially compensated for SOC loss during land conversion (O'riordan et al., 2021). Because the construction materials could add large amounts of inorganic C into soil, it is preferable to investigate the C:N stoichiometry under ISAs with the SOC:N ratio rather than the total C:total N ratio. This study highlights the important role of N in urban biogeochemical research, which helps to prevent us from being confused/misled by the complex C dynamics in urban soil due to anthropogenic C inputs.

5.3 Potential driving factors of the N_{ISA} and $SOC:N_{ISA}$

Similar to natural ecosystem soils, the spatial distribution pattern of N_{ISA} was significantly correlated with climate factors such as temperature and precipitation (Yang et al., 2007). In northern China, N_{ISA} increased from arid to humid zones and was thus positively correlated with precipitation, and in eastern China, it increased from temperate to cold temperate zones and was thus negatively correlated with temperature. The dynamics of soil N under impervious surfaces could be influenced by many factors, such as the pre–conversion N content, the N mineralization rate, the denitrification rate and the N leaching rate during or after land conversion (Zhang et al., 2023). All these factors are influenced by net primary ecosystem productivity (NPP) and climate factors (Epstein et al., 2002). As a result, the pattern of N_{ISA} could be complex and difficult to explain.

The soil C:N ratio could be a more stable parameter (Yang et al., 2021). It has been observed that the soil stoichiometric characteristics in China are influenced by geographical parameters such as altitude and latitude (Sheng et al., 2022). Lu et al. (2023) found a lower SOC:N ratio at higher latitudes in China, suggesting a positive correlation between SOC:N and temperature in natural ecosystem soils (Lu et al., 2023). Our study, however, found that the $SOC:N_{ISA}$ ratio increased with latitude and that there was a significant negative

correlation between the SOC:N_{ISA} ratio and temperature. The soil C:N ratio of natural ecosystems is influenced by plant litter input and N uptake. Ecosystems in warmer regions have higher NPP, resulting in

285   higher inputs of litter with a high C:N ratio (compared with the soil C:N ratio) and higher N uptake by roots, thus reducing soil inorganic N. Therefore, the SOC:N ratio is positively correlated with temperature in natural ecosystems. However, the SOC:N ratio under the impervious surface is solely determined by the relative mineralization rate of C and N. It seems that soil ecosystems have a higher retention capacity for N than for C (C fixation is unlikely to be found in sealed soil). Therefore, while both the soil N_{ISA} pool and the SOC_{ISA}

290   pool decrease when the temperature increases, the net N mineralization rate is lower than the C mineralization rate, leading to a negative correlation between the SOC:N_{ISA} ratio and temperature.

5.4 Potential applications of the data

Soil microbial C use efficiency is negatively correlated with SOC:N (Schroeder et al., 2022). Incorporating N into Earth system models can improve the accuracy of C cycle estimates (Fleischer et al., 2019), and a

295   good description of N can help understand and predict the patterns and mechanisms of global C dynamics (Zhang et al., 2021) and provide a reliable basis for exploring how geochemical cycles are coupled.

For a long time, knowledge of biogeochemical cycles under impervious surfaces has been a major gap in urban biogeochemical research. Until now, the size and pattern of N_{ISA} pools and their contributions to the global N cycle have remained unclear. Our research, which is the first national–scale study on N_{ISA} and

300   SOC:N_{ISA}, helps to fill this gap by improving our understanding of the special pattern of soil N under impervious surfaces. Such information is necessary when assessing urbanization impacts on global C and N cycles (Lorenz and Lal, 2009).

Author contributions. Conceptualization: CZ. Data curation: CZ. Formal analysis: QD. Funding acquisition: ZC and HS. Investigation: HS. and XF. Methodology: QD and CZ. Project administration: CZ and HS.

305   Resources: HS. and XF. Software: QD. Supervision: CZ. Validation: QD. Visualization: QD. Writing – original draft preparation: QD. Writing – review & editing: QD., HS. and CZ.

Competing interests. The authors declare that they have no conflicts of interest.

Acknowledgements. This project was funded by the National Natural Science Foundation of China (Grant 31770515). Chi Zhang is supported by the Taishan Scholars Program of Shandong, China (Grant

310   ts201712071).

References

Bae, J. and Ryu, Y.: High soil organic carbon stocks under impervious surfaces contributed by urban deep cultural layers, Landscape and Urban Planning, 204, https://doi.org/10.1016/j.landurbplan.2020.103953, 2020.

315   Bremner, J. and Mulvaney, C.: Methods of Soil Analysis. Part 2. Chemical and Microbiological Properties, Nitrogen-Total, American Society of Agronomy, Soil Science Society of America, 595–624 pp.1982.

Cambou, A., Shaw, R. K., Huot, H., Vidal-Beaudet, L., Hunault, G., Cannavo, P., Nold, F., and Schwartz, C.: Estimation of soil organic carbon stocks of two cities, New York City and Paris, Sci. Total Environ., 644, 452-464, https://doi.org/10.1016/j.scitotenv.2018.06.322, 2018.

320 Chapin, F. S., Matson, P. A., and Vitousek, P. M.: Principles of Terrestrial Ecosystem Ecology, Springer, New York2011.

Ding, Q., Shao, H., Chen, X., and Zhang, C.: Urban Land Conversion Reduces Soil Organic Carbon Density Under Impervious Surfaces, Global Biogeochemical Cycles, 36, e2021GB007293, https://doi.org/10.1029/2021GB007293, 2022.

325 Ding, Q., Shao, H., Zhang, C., and Fang, X.: Observations of soil nitrogen and soil organic carbon to soil nitrogen stoichiometry under the impervious surfaces areas (ISA) of China, National Cryosphere Desert Data Center, https://doi.org/10.12072/ncdc.socn.db2851.2023, 2023.

Epstein, H. E., Burke, I. C., and Lauenroth, W. K.: Regional patterns of decomposition and primary production rates in the U.S. great plains, Ecology, 83, 320-327, https://doi.org/10.1890/0012-
330 9658(2002)083[0320:RPODAP]2.0.CO;2, 2002.

Fleischer, K., Rammig, A., De Kauwe, M. G., Walker, A. P., Domingues, T. F., Fuchslueger, L., Garcia, S., Goll, D. S., Grandis, A., Jiang, M., Haverd, V., Hofhansl, F., Holm, J. A., Kruijt, B., Leung, F., Medlyn, B. E., Mercado, L. M., Norby, R. J., Pak, B., von Randow, C., Quesada, C. A., Schaap, K. J., Valverde-Barrantes, O. J., Wang, Y.-P., Yang, X., Zaehle, S., Zhu, Q., and Lapola, D. M.: Amazon forest response to CO2
335 fertilization dependent on plant phosphorus acquisition, Nature Geoscience, 12, 736-741, https://doi.org/10.1038/s41561-019-0404-9, 2019.

Fowler, D., Coyle, M., Skiba, U., Sutton, M. A., Cape, J. N., Reis, S., Sheppard, L. J., Jenkins, A., Grizzetti, B., Galloway, J. N., Vitousek, P., Leach, A., Bouwman, A. F., Butterbach-Bahl, K., Dentener, F., Stevenson, D., Amann, M., and Voss, M.: The global nitrogen cycle in the twenty-first century, Philosophical
340 Transactions of the Royal Society B: Biological Sciences, 368, 20130164, https://doi.org/10.1098/rstb.2013.0164, 2013.

Gao, D., Bai, E., Wang, S., Zong, S., Liu, Z., Fan, X., Zhao, C., and Hagedorn, F.: Three-dimensional mapping of carbon, nitrogen, and phosphorus in soil microbial biomass and their stoichiometry at the global scale, Global Change Biology, 28, 6728-6740, https://doi.org/10.1111/gcb.16374, 2022.

345 Hu, Y., Dou, X., Li, J., and Li, F.: Impervious Surfaces Alter Soil Bacterial Communities in Urban Areas: A Case Study in Beijing, China, Frontiers in Microbiology, 9, https://doi.org/10.3389/fmicb.2018.00226, 2018.

Kuang, W.: Mapping global impervious surface area and green space within urban environments, Science China-Earth Sciences, 62, 1591-1606, https://doi.org/10.1007/s11430-018-9342-3, 2019.

Kuhn, M.: Classification and Regression Training [R package caret version 6.0-86],

350 Lehmann, A. and Stahr, K.: Nature and significance of anthropogenic urban soils, J. Soils Sediments, 7, 247-260, https://doi.org/10.1065/jss2007.06.235, 2007.

Li, S.-L., Liu, X., Yue, F.-J., Yan, Z., Wang, T., Li, S., and Liu, C.-Q.: Nitrogen dynamics in the Critical Zones of China, Progress in Physical Geography: Earth and Environment, 46, 869-888, https://doi.org/10.1177/03091333221114732, 2022.

355 Liaw, A. and Wiener, M.: Classification and Regression by randomForest, R News, 23, 2002.

Lorenz, K. and Lal, R.: Biogeochemical C and N cycles in urban soils, Environment International, 35, 1-8, https://doi.org/10.1016/j.envint.2008.05.006, 2009.

Lu, M., Zeng, F., Lv, S., Zhang, H., Zeng, Z., Peng, W., Song, T., Wang, K., and Du, H.: Soil C:N:P stoichiometry and its influencing factors in forest ecosystems in southern China, Frontiers in Forests and
360 Global Change, 6, https://doi.org/10.3389/ffgc.2023.1142933, 2023.

Majidzadeh, H., Lockaby, B. G., and Governo, R.: Effect of home construction on soil carbon storage-A chronosequence case study, Environmental Pollution, 226, 317-323, https://doi.org/10.1016/j.envpol.2017.04.005, 2017.

O'Riordan, R., Davies, J., Stevens, C., and Quinton, J. N.: The effects of sealing on urban soil carbon and
365 nutrients, SOIL, 7, 661-675, https://doi.org/10.5194/soil-7-661-2021, 2021.

Pereira, M. C., O'Riordan, R., and Stevens, C.: Urban soil microbial community and microbial-related carbon storage are severely limited by sealing, J. Soils Sediments, 21, 1455-1465, https://doi.org/10.1007/s11368-021-02881-7, 2021.

Piotrowska-Długosz, A. and Charzyński, P.: The impact of the soil sealing degree on microbial biomass,
370 enzymatic activity, and physicochemical properties in the Ekranic Technosols of Toruń (Poland), J. Soils Sediments, 15, 47-59, https://doi.org/10.1007/s11368-014-0963-8, 2015.

Pouyat, R. V., Russell-Anelli, J., Yesilonis, I. D., and Groffman, P. M.: Soil carbon in urban forest ecosystems, in: Potential of U.S. Forest Soils to Sequester Carbon and Mitigate the Greenhouse Effect, CRC Press, 347-362, 2003.

375 Raciti, S. M., Hutyra, L. R., and Finzi, A. C.: Depleted soil carbon and nitrogen pools beneath impervious surfaces, Environmental Pollution, 164, 248-251, https://doi.org/10.1016/j.envpol.2012.01.046, 2012.

Schroeder, J., Peplau, T., Pennekamp, F., Gregorich, E., Tebbe, C. C., and Poeplau, C.: Deforestation for agriculture increases microbial carbon use efficiency in subarctic soils, Biology and Fertility of Soils, https://doi.org/10.1007/s00374-022-01669-2, 2022.

380 Seto, K. C., Guneralp, B., and Hutyra, L. R.: Global forecasts of urban expansion to 2030 and direct impacts on biodiversity and carbon pools, Proceedings of the National Academy of Sciences of the United States of America, 109, 16083-16088, https://doi.org/10.1073/pnas.1211658109, 2012.

Shcherbakov, M., Brebels, A., Shcherbakova, N. L., Tyukov, A., Janovsky, T. A., and Kamaev, V. A.: A survey of forecast error measures, World Applied Sciences Journal, 24, 171-176, 385 https://doi.org/10.5829/idosi.wasj.2013.24.itmies.80032, 2013.

Sheng, H., Yin, Z., Zhou, P., and Thompson, M. L.: Soil C:N:P ratio in subtropical paddy fields: variation and correlation with environmental controls, J. Soils Sediments, 22, 21-31, https://doi.org/10.1007/s11368-021-03046-2, 2022.

Short, J. R., Fanning, D. S., Foss, J. E., and Patterson, J. C.: SOILS OF THE MALL IN WASHINGTON, 390 DC .2. GENESIS, CLASSIFICATION, AND MAPPING, Soil Science Society of America Journal, 50, 705-710, https://doi.org/10.2136/sssaj1986.03615995005000030031x, 1986.

Tang, X., Zhao, X., Bai, Y., Tang, Z., Wang, W., Zhao, Y., Wan, H., Xie, Z., Shi, X., Wu, B., Wang, G., Yan, J., Ma, K., Du, S., Li, S., Han, S., Ma, Y., Hu, H., He, N., Yang, Y., Han, W., He, H., Yu, G., Fang, J., and Zhou, G.: Carbon pools in China's terrestrial ecosystems: New estimates based on an intensive field survey, 395 Proceedings of the National Academy of Sciences, 115, 4021-4026, https://doi.org/10.1073/pnas.1700291115, 2018.

Tian, H., Chen, G., Zhang, C., Melillo, J. M., and Hall, C. A. S.: Pattern and variation of C:N:P ratios in China's soils: a synthesis of observational data, Biogeochemistry, 98, 139-151, https://doi.org/10.1007/s10533-009-9382-0, 2010.

400 Tian, H., Wang, S., Liu, J., Pan, S., Chen, H., Zhang, C., and Shi, X.: Patterns of soil nitrogen storage in China, Global Biogeochemical Cycles, 20, https://doi.org/10.1029/2005GB002464, 2006.

Vitousek, P. M. and Howarth, R. W.: Nitrogen limitation on land and in the sea: How can it occur?, Biogeochemistry, 13, 87-115, https://doi.org/10.1007/BF00002772, 1991.

Wei, Z., Wu, S., Yan, X., and Zhou, S.: Density and Stability of Soil Organic Carbon beneath Impervious 405 Surfaces in Urban Areas, Plos One, 9, https://doi.org/10.1371/journal.pone.0109380, 2014a.

Wei, Z., Wu, S., Zhou, S., and Lin, C.: Installation of impervious surface in urban areas affects microbial biomass, activity (potential C mineralisation), and functional diversity of the fine earth, Soil Research, 51, 59-67, https://doi.org/10.1071/sr12089, 2013.

Wei, Z., Wu, S., Zhou, S., Li, J., and Zhao, Q.: Soil Organic Carbon Transformation and Related Properties 410 in Urban Soil Under Impervious Surfaces, Pedosphere, 24, 56-64, https://doi.org/10.1016/s1002-0160(13)60080-6, 2014b.

Xu, L., He, N., and Yu, G.: Nitrogen storage in China's terrestrial ecosystems, Sci. Total Environ., 709, 136201, https://doi.org/10.1016/j.scitotenv.2019.136201, 2020.

Yan, Y., Kuang, W., Zhang, C., and Chen, C.: Impacts of impervious surface expansion on soil organic 415 carbon - a spatially explicit study, Sci Rep, 5, https://doi.org/10.1038/srep17905, 2015.

Yang, J.-L., Yuan, D.-G., Zhao, Y.-G., He, Y., and Zhang, G.-L.: Stoichiometric relations of C, N, and P in urban top soils in Nanjing, China, and their biogeochemical implications, J. Soils Sediments, 21, 2154-2164, https://doi.org/10.1007/s11368-020-02826-6, 2021.

Yang, Y., ma, W., Mohammat, A., and Fang, J.-Y.: Storage, Patterns and Controls of Soil Nitrogen in China, 420 Pedosphere, 17, 776-785, https://doi.org/10.1016/S1002-0160(07)60093-9, 2007.

Yu, W. W., Hu, Y. H., Cui, B. W., Chen, Y. Y., and Wang, X. K.: The Effects of Pavement Types on Soil Bacterial Communities across Different Depths, Int. J. Environ. Res. Public Health, 16, 11, https://doi.org/10.3390/ijerph16101805, 2019.

Zhang, K., Qiu, Y., Zhao, Y., Wang, S., Deng, J., Chen, M., Xu, X., Wang, H., Bai, T., He, T., Zhang, Y., 425 Chen, H., Wang, Y., and Hu, S.: Moderate precipitation reduction enhances nitrogen cycling and soil nitrous oxide emissions in a semi-arid grassland, Global change biology, https://doi.org/10.1111/gcb.16672, 2023.

Zhang, X., Liu, L., Wu, C., Chen, X., Gao, Y., Xie, S., and Zhang, B.: Development of a global 30-m impervious surface map using multisource and multitemporal remote sensing datasets with the Google Earth Engine platform, Earth Syst. Sci. Data, 12, 1625-1648, https://doi.org/10.5194/essd-12-1625-2020, 2020.

430 Zhang, Y. W., Guo, Y., Tang, Z., Feng, Y., Zhu, X., Xu, W., Bai, Y., Zhou, G., Xie, Z., and Fang, J.: Patterns of nitrogen and phosphorus pools in terrestrial ecosystems in China, Earth Syst. Sci. Data, 13, 5337-5351, https://doi.org/10.5194/essd-13-5337-2021, 2021.

Zhao, D., Li, F., Wang, R., Yang, Q., and Ni, H.: Effect of soil sealing on the microbial biomass, N transformation and related enzyme activities at various depths of soils in urban area of Beijing, China, J. Soils

435 Sediments, 12, 519-530, https://doi.org/10.1007/s11368-012-0472-6, 2012.

Zhao, H., Wu, S., Xu, X., Zhou, S., and Li, X.: Spatial Distribution of Soil Inorganic Carbon in Urban Soil and Its Relationship with Urbanization History of the City, Acta Pedologica Sinica, 54, 1540-1546, https://doi.org/10.11766/trxb201703300075, 2017.